Polymer Chemistry

Accepted Manuscript

This is an *Accepted Manuscript*, which has been through the Royal Society of Chemistry peer review process and has been accepted for publication.

Accepted Manuscripts are published online shortly after acceptance, before technical editing, formatting and proof reading. Using this free service, authors can make their results available to the community, in citable form, before we publish the edited article. We will replace this *Accepted Manuscript* with the edited and formatted *Advance Article* as soon as it is available.

You can find more information about *Accepted Manuscripts* in the Information for Authors.

Please note that technical editing may introduce minor changes to the text and/or graphics, which may alter content. The journal's standard Terms & Conditions and the Ethical guidelines still apply. In no event shall the Royal Society of Chemistry be held responsible for any errors or omissions in this *Accepted Manuscript* or any consequences arising from the use of any information it contains.

ROYAL SOCIETY OF CHEMISTRY

www.rsc.org/polymers

Towards Sugar-Derived Polyamides as Environmentally Friendly Materials

Aleksandra Wroblewska,[a] Arkadiusz Zych,[a] Shanmugam Thiyagarajan,[b] Dmytro Dudenko,[c] Daan van Es,[b] Michael Ryan Hansen,[c,d] Cor Koning,[e] Rob Duchateau,[*e] Lidia Jasinska-Walc[*a,e]

Received (in XXX, XXX) Xth XXXXXXXXX 20XX, Accepted Xth XXXXXXXXX 20XX
DOI: 10.1039/b000000x

As part of our ongoing study investigating isohexide-based polyamides we have synthesized isosorbide(bis(propan-1-amine)) (DAPIS) and studied its reactivity in the polymerization towards fully biobased polyamides. Polycondensation of nylon salts with various contributions of DAPIS afforded a family of homo- and copolyamides, which were characterized using complementary spectroscopic techniques. The chemical structure of the materials was determined by FT-IR, 1D and 2D liquid-state NMR spectroscopy, whilst the supramolecular arrangement, conformational changes upon heating, and molecular mobility of the polymers were investigated by solid-state $^{13}C\{^{1}H\}$ Cross-Polarization/Magic-Angle Spinning (CP/MAS) NMR and $^{13}C\{^{1}H\}$ Insensitive Nuclei Enhanced by Polarization Transfer (INEPT) experiments. The abundance of the different DAPIS conformers was determined by DFT-D computational methods. The thermal properties of the polyamides were tested for polymers with different amounts of isohexide units in the backbone by DSC and TGA, demonstrating that increasing amounts of isohexide diamine efficiently decreases their melting point and slightly their thermal stability. The relaxation processes of the isohexide-derived polyamides were studied by DMTA.

Introduction

A rapidly depleting fossil feedstock has stimulated extensive research in biobased monomers used for the synthesis of polymeric materials.[1-5] Biomass offers a plethora of carbohydrates, however, their limited thermal stability, caused by the presence of various reactive functional groups, is a major drawback. Reducing the number of functional groups and preparation of bifunctional monomers is therefore under attention of many researchers,[6-7] and has resulted in more stable, biobased building blocks like furan-2,5-dicarboxylic acid,[8-9] succinic acid,[10] levulinic acid[11-13] and 1,4:3,6-dianhydrohexides.[14,15] Their unique chemical structure consisting of a bicyclic fragment, chirality and diverse reactivity, make the isohexide derivatives interesting monomer building blocks for the production of high glass transition temperature (T_g) biobased polymers.[16-19] The isohexides can be prepared from C6-alditols such as sorbitol or mannitol via acid catalyzed cyclodehydration, affording 1,4;3,6-dianhydro-D-glucidol (isosorbide), 1,4;3,6-dianhydro-D-mannitol (isomannide) or 1,4;3,6-dianhydro-L-iditol (isoidide).[19]

Despite the limited reactivity of the secondary hydroxyl groups and the possibility of intramolecular hydrogen bond formation when using isosorbide and isomanide as monomers during the condensation polymerization,[20-21] it turned out that isohexides perform well when used in the presence of non-rigid building blocks, for instance, ethylene glycol or 1,4-butanediol in combination with terephthalate esters. Polyesters containing dianhydroisosorbitols revealed increased glass transition temperature and preserved crystallinity, making them very suitable blow molding or thermoforming products. Related to this, it also proved possible to replace terephthalic acid by isohexide-derivatives leading to fully biobased materials.[22-23] Furthermore, taking the chemical structure and the corresponding properties into account, they can successfully replace bisphenol-A in the production of polycarbonates.[19] Recently Munoz-Guerra et al. presented an interesting class of polyesters based on bicyclic carbohydrate-derived compounds.[24-30] By using building blocks having primary functionalities e.g. 2,4:3,5-di-*O*-methylene-D-mannitol or 2,4:3,5-di-*O*-methylene-D-glucitol relatively high molecular weights of the synthesized polymers were achieved. As pointed out by the researchers, fine-tuning of the polyesters' compositions and microstructures led not only to sustainable materials but also to the products having glass transition temperature exceeding 130 °C.

In an effort to efficiently produce isohexide-derived polyamides, Thiem[2] and Bartolussi[31] have reported interfacial polymerization and microwave-assisted polymerization, respectively. Although these isohexide-based polyamides showed interesting properties, the abovementioned synthetic approaches are not applicable on an industrial scale. Therefore, the challenge is to find an economically viable route to prepare such isohexide-based polyamides, exhibiting a relatively high molecular weight under solvent-free conditions.

Recently, we developed efficient routes towards a family of isohexide-derived polyamides based on diamines having *exo-endo* and *exo-exo* configuration viz. 2,5-diamino-2,5-dideoxy-1,4;3,6-dianhydrosorbitol[32] and 2,5-diamino-2,5-dideoxy-1,4;3,6-dianhydroiditol[33-34] as well as its primary homologue isoidide-2,5-dimethyleneamine.[35] It was proven that the latter one reveals a significantly higher reactivity in comparison to its secondary analogues. Inspired by these exploratory studies on isohexide derivatives, in this work we have established an efficient synthetic pathway towards new isosorbide(bis(propan-1-amine)) (DAPIS), a sterically less hindered and therefore more reactive isohexide-derived primary diamine. The corresponding polymers were synthesized via melt polymerization followed by solid-state post-condensation and their properties were compared with those

of polyamides consisting of secondary isohexide-based diamines. The products were thoroughly characterized with respect to their chemical structure, conformation, performance and thermal properties.

Experimental

Materials

Sebacic acid (SA, 99 %), suberic acid (SubA, 98 %), suberoyl chloride (99 %), 1,11-undecanedicarboxylic acid (BrA, 94 %), 1,4-diaminobutane (DAB, 99 %), 1,6-diaminohexane (DAH, 99 %), 1,4;3,6-dianhydro-D-sorbitol (isosorbide, DAIS 98 %), 1,4:3,6-dianhydro-D-mannitol (isomannide, 99 %), p-toluenesulfonyl chloride (99 %), potassium phthalimide (99 %), dimethyl sulfoxide (99.9 %), 3-bromopropionitrile (99 %), borane tetrahydrofuran complex (1M solution in THF), hydrochloric acid (reagent grade 37 %), ethanolic hydrochloric acid solution (1.25 N), Amberlyst A26-OH, *N,N*-dimethylformamide (99 %), potassium carbonate (99 %), CD_3Cl (99.8 atom %D), and C_6D_6 (99 atom %D) were purchased from Sigma-Aldrich. Irganox 1330 was available from Ciba Specialty Chemicals. Magnesium sulphate (99 %) was purchased from Acros Organics. Acetic acid (glacial, 99-100 %), pyridine (99.5 %), and D_2O (99.8 atom %D) were purchased from Merck. CF_3CO_2D (99.5 atom %D) was purchased from Cambridge Isotope Laboratories, Inc. Activated carbon was purchased from Norit. 1,1,1,3,3,3-Hexafluoro-2-propanol (HFIP), diethyl ether, methanol, ethanol, and dry chloroform were purchased from Biosolve. All the chemicals were used as received, unless denoted otherwise. 2,5-Diamino-1,5-dideoxy-1,4;3,6-dianhydrosorbitol (diaminoisosorbide) and 2,5-diamino-2,5-dideoxy-1,4;3,6-dianhydroiditol (diaminoisoidide) were synthesized according to the procedure reported by Thiyagarajan et al.[36]

3,3'-(((3R,6S)-hexahydrofuro[3,2-b]furan-3,6-diyl)bis(oxy))dipropanenitrile (Scheme S1).

A 500 mL three-necked round-bottom flask, equipped with a magnetic stirrer, pressure equalizing dropping funnel and a reflux condenser was charged with isosorbide (15.0 g, 0.10 mol) and K_2CO_3 (56.6 g, 0.41 mol), followed by dry DMF (175 mL) under continuous flow of nitrogen. The suspension was stirred at 70 °C for 3 h. 3-Bromopropionitrile (26 ml, 0.30 mol) was added dropwise into the reaction mixture over a period of 1.5 h. The reaction was further allowed to stir at 70 °C for 48 h. After cooling to room temperature, the mixture was poured into cold water (1.0 L) with constant stirring. The crude product was extracted from the aqueous phase using chloroform (3 × 300 mL). The combined extracts were dried over magnesium sulfate, filtered and evaporated under reduced pressure using a rotatory evaporator affording the crude product (yield: 19.0 g, 75 mmol). The pure isosorbide-extended dinitrile was obtained as a colorless oily liquid by short-path distillation using a kugelrohr glass oven at 165 °C, under vacuum of 0.02 mbar for 2.0 h (yield: 16.5 g, 63 %). ^{1}H NMR (400 MHz, $CDCl_3$, δ ppm): 4.71 (t, 1H), 4.52 (d, 1H), 3.99 (m, 6H), 3.74 (m, 4H), 2.66 (m, 4H); $^{13}C\{^1H\}$ NMR (100 MHz, $CDCl_3$, δ ppm): 117.65, 117.54, 85.99, 84.31, 80.53, 80.32, 73.00, 70.64, 65.08, 64.05, 18.95.

3,3'-(((3R,6S)-hexahydrofuro[3,2-b]furan-3,6-diyl)bis(oxy))-bis(propan-1-amine)—isosorbide(bis(propan-1-amine)) (Scheme S1).

A 250 mL three-necked round-bottom flask, equipped with a magnetic stirrer, pressure equalizing dropping funnel and a reflux condenser was charged with BH_3·THF complex in THF solution (1.0 M, 100 mL). Next, during 1 h a solution of 3,3'-(((3R,6S)-hexahydrofuro[3,2-b]furan-3,6-diyl)bis(oxy))dipropanenitrile (10.0 g, 0.039 mol) in THF (75 mL) was added dropwise at room temperature under a nitrogen flow. After the addition was completed, the reaction was stirred for another 18 h. Then, methanol (50 mL) was added carefully to quench the reaction, during which hydrogen gas evolved vigorously. Once the gas formation had ceased, hydrochloric acid in diethyl ether solution (2.0 M, 100 mL) was added dropwise upon which a white precipitate formed. The suspension was then filtered over a glass filter (G-3), and dried in an oven (70 °C, 1 atm.) for 3 h, to give the crude diamine·HCl salt (11.2 g, 34 mmol, 85 %) as white powder. The diamine·HCl salt (11.0 g, 0.033 mol) was dissolved in demineralized water (100 mL) giving a colorless solution. To this solution freshly washed Amberlyst A 26-OH (55 g) was added. The resulting suspension was sonificated in an ultrasonic bath for 1.5 h at 30 °C. After the reaction was completed, the suspension was filtered over a glass filter (G-3) containing Celite and the resin was washed thoroughly with water (3 × 20 mL). The combined clear colorless solutions were evaporated to dryness using a rotary evaporator to afford the extended diamine as a colorless oily liquid. The crude product was purified further by distillation using a kugelrohr glass oven at 160 °C under vacuum of 0.02 mbar for 2 h (yield: 8.2 g, 32 mmol, 95 %, purity 99 % based on NMR and GC analyses). ^{1}H NMR (400 MHz, CD_3OD, δ ppm): 4.64 (t, ^{1}H), 4.49 (d, 1H), 4.01 (m, 1H), 3.91 (m, 4H), 3.71 (m, 1H), 3.52 (m, 4H), 2.71 (m, 4H), 1.71 (m, 4H); $^{13}C\{^1H\}$ NMR (100 MHz, CD_3OD, δ ppm): 87.42, 85.67, 81.66, 81.52, 74.23, 71.24, 69.50, 68.69, 39.95, 39.94, 33.79, 33.56.

Diaminoisoidide-suberic acid salt.

To a solution of suberic acid (2.6 g, 0.015 mol) in ethanol (10 mL) at 50 °C a solution of diaminoisoidide (2.2 g, 0.015 mol) in an ethanol/water mixture (6 mL, 5:1, v/v) was added dropwise. During the addition, a precipitate was formed. The mixture was stirred at 80 °C for 2 h. The crude product was filtered and recrystallized from an ethanol/water mixture (8:1, v/v) to afford the salt as white crystals (4.7 g, 11 mmol, 86 %). ^{1}H NMR (D_2O): δ = 4.84 (s, 2H), 4.05 (dd, 2H), 3.89 (d, 2H), 3.86 (m, 2H), 2.12 (m, 4H), 1.42 (m, 4H), 1.17 (m, 6H).

Diaminoisosorbide-suberic acid salt, 1,4-diaminobutane-suberic acid salt, 1,4-diaminobutane-sebacic acid salt, 1,4-diaminobutane-undecanedicarboxylic acid salt, 1,6-diamonohexane-suberic acid salt, 1,6-diamonohexane-sebacic acid salt, 1,6-diamonohexane-1,11-undecanedicarboxylic acid salt were synthesized according to the procedure presented above.

Isosorbide(bis(propan-1-amine))-suberic acid salt.

To a solution of suberic acid (2.6 g, 0.015 mol) in ethanol (10 mL) at 50 °C a solution of isosorbide(bis(propan-1-amine)) (3.9 g, 0.015 mol) in ethanol (6 mL) was added dropwise. The mixture was stirred at 80 °C for 2 h. The solvent was removed under reduced pressure. The product was obtained as an oil. ^{1}H NMR (D_2O): δ = 4.84 (s, 2H), 4.05 (dd, 2H), 3.89 (d, 2H), 3.86 (m, 2H), 2.12 (m, 4H), 1.42 (m, 4H), 1.17 (m, 6H).

Isosorbide(bis(propan-1-amine))-sebacic acid salt and isosorbide(bis(propan-1-amine))-undecanedicarboxylic acid salt were synthesizes according to the procedure presented above.

Polymerization of nylon salts.

This example is representative for all conducted homo- and copolymerizations of nylon salts. A mixture of isosorbide(bis(propan-1-amine))-sebacic acid salt (0.66 g, 1,43 mmol) and 1,4-diaminobutane-sebacic acid salt (2.0 g, 6,86 mmol), 1,4-diaminobutane (0.2 g, 2.3 mmol), isosorbide(bis(propan-1-amine)) (0.066 g, 0.25 mmol) was stirred in a three-necked round-bottom flask equipped with a mechanical stirrer and vigreux column. The reaction mixture was heated under nitrogen atmosphere at 160 °C for 0.5 h and then the temperature was raised to 190 °C and the reaction was continued for an additional 1.5 h. The polycondensation process was conducted in the presence of Irganox 1330 (0.026 g) as an antioxidant. The low molecular weight polyamide was ground into powder, washed with demineralized water at 80 °C for 12 h, filtered, and dried under reduced pressure at 80 °C. In order to increase the molecular weight of the polyamide prepolymers, solid-state polymerization (SSP) was applied. SSP of the polyamide powder was carried out in a glass tube reactor (2.5 cm diameter) equipped with a sintered glass plate at the bottom on which the polyamide prepolymer powder was deposited. During the reaction course, the temperature was raised gradually to 180 °C for 27 h and maintained 10-15 °C below the melting point of the polyamide prepolymer. The reactor was heated using a salt mixture of KNO_3 (53 wt %), $NaNO_2$ (40 wt %), $NaNO_3$ (7 wt %). SSP was carried out in N_2 atmosphere at a gas flow rate of 2.5 L/min.

Interfacial polycondensation.

To a solution of isosorbide(bis(propan-1-amine)) (0.325 g, 1.25 mmol) and potassium carbonate (0.69 g, 5 mmol) in water (15 mL) a solution of suberoyl chloride (0.263 g, 1.25 mmol) in dry chloroform (5 mL) was added dropwise. The heterogeneous mixture was stirred at room temperature for 2 h under nitrogen atmosphere. The synthesized polyamide was filtered, washed with water, ethanol, and dried under reduced pressure at 50 °C (0.43 g, 86%). ^{1}H NMR (CF_3COOD): δ = 7.78 (s, 1H), 4.34 (s, 1H), 3.79 (m, 1H), 3.77 (m, 1H), 3.75 (m, 4H), 3.69 (m, 4H), 2.34 (m, 4H), 2.07 (m, 4H), 1.58 (m, 4H), 1.44 (m, 4H).

Characterization of copolymers.

Size exclusion chromatography analyses (SEC) in 1,1,1,3,3,3-hexafluoro-2-propanol were performed using a setup equipped with a Shimadzu LC-10AD pump and a waters 2414 differential refractive index detector. PSS (2 x PFG-lin-XL, 7 µm, 8 × 300 mm) columns were used. The eluent flow rate was 1.0 mL/min. Calibration of the measurements was carried out with PMMA standards. The data acquisitions were performed using Viscotek OmniSec 4.0 and Waters Empower 2.0 software.

2D NMR spectra were recorded on a Varian Unity 500 plus spectrometer at room temperature. Chemical shifts were referenced to residual signals of C_6D_6. Correlation spectra (COSY) were acquired using standard programs provided by a Varian spectrometer library with the following parameters: spectral width SW1 = SW2 = 6075.3 Hz, acquisition time 0.221 s, relaxation delay 1.4 s, and number of scans 8 × 300 increments. ^{1}H NMR and ^{13}C{^{1}H} NMR spectra were recorded using a Varian Mercury Vx spectrometer at a frequency of 400 MHz. For ^{1}H NMR experiments the spectral width was 6402.0 Hz, acquisition time 1.998 s, and the number of recorded scans equal to 64. ^{13}C{^{1}H} NMR spectra were recorded with the spectral width 24154.6 Hz, acquisition time 1.300 s, and the minimum number of recorded scans equal to 256.

DSC measurements were performed using a DSC Q100 from TA Instruments. The measurements were carried out in a nitrogen atmosphere with a heating rate of 10 °C/min. The transitions were deduced from the second heating and cooling curves.

Fourier transform infrared spectra (FT-IR) were obtained using a Varian 610-IR spectrometer equipped with an FT-IR microscope. The spectra were recorded at 30 °C in transmission mode with a resolution of 2 cm^{-1}. PA films obtained from HFIP were analyzed on a zinc selenium disk.

Geometry optimization and ^{13}C NMR chemical shift calculations were performed within the Gaussian03 program package.[37a] The geometries of the conformations obtained by merging results from a set of independent one-dimensional potential energy surface (1D-PES) scanning procedures via B97-D/6-311G** level of theory with Grimme dispersion correction[37b] were further fully optimized at the same level in the gas phase. The most abundant conformers with respect to the Gibbs free energy have been proceeded for further NMR chemical shifts calculations at the B97-D/6-311G** level of theory. Additionally, for all conformers found a vibrational frequency analysis was carried out to ensure that all described geometries are at local minima (not saddle points).

Solid-State NMR. Variable-Temperature (VT) solid-state ^{13}C{^{1}H} Cross-Polarization/Magic-Angle Spinning (CP/MAS) NMR and ^{13}C{^{1}H} Insensitive Nuclei Enhanced by Polarization Transfer (INEPT) experiments were carried out on a Bruker AVANCE III 500 spectrometer employing a double-resonance H-X probe for rotors with 4.0 mm outside diameter. These experiments utilized a MAS frequency of 10.0 kHz, a 5.0 µs π/2 pulse for ^{1}H and ^{13}C, a CP contact time of 2.0 ms and TPPM decoupling during acquisition. The CP conditions were pre-optimized using L-alanine. The ^{13}C{^{1}H} INEPT spectra were recorded using the refocused-INEPT sequence with a *J*-evolution period of either $1/(3J_{CH})$ or $1/(6J_{CH})$ assuming a $^1J_{CH}$ of 150 Hz, i.e. for a *J*-evolution time of $1/3\ J_{CH}$ the signals from CH and CH_3 groups are positive, while those of CH_2 are negative.[38-40] The VT ^{13}C{^{1}H} CP/MAS and ^{13}C{^{1}H} INEPT MAS NMR spectra were recorded under isothermal conditions at selected temperatures. A heating rate of 2 °C/min was employed between temperatures. Reported temperatures are corrected for friction-induced heating due to spinning using ^{207}Pb MAS NMR of $Pb(NO_3)_2$ as a NMR thermometer.[41-43] Chemical shifts for ^{1}H and ^{13}C are reported relative to TMS using solid adamantane as an external.[44]

Thermogravimetric analysis (TGA) was performed on a TGA Q1000 from TA Instruments. The measurements were carried out in a nitrogen atmosphere. Samples were heated from 20 to 600 ºC with a scan rate 10 ºC/min.

Dynamic mechanical thermal analysis (DMTA) was performed using a DMAQ800 (TA) in tensile film mode. The dimensions of the specimen were 30 x 4 x 0,05 mm. The solvent casted samples were measured from -140 to 200 $^{\circ}$C at a heating rate of 3 ^{0}C /min and at a frequency of 1Hz with a constant amplitude of 10 μ m.

Table 1. Overview of the chemical composition, molecular weight and thermal properties of the synthesized polyamides.

entry	Composition[a]	M_n before SSP[b] (g/mol)	PDI[b]	M_n after SSP[b] (g/mol)	PDI[b]	T_m[c] (°C)	ΔH_m[c] (J/g)
PA1	C8/DAB	8800	2.1	18700	2.5	260	89
PA2	C8/DAB/30%DAIS	8460	2.5	10500	3.2	234	43
PA3	C8/DAB/15%DAIS/15%DAII	19200	2.8	32600	3.0	230	42
PA4	C8/DAB/30%DAII	6800	2.8	8400	3.1	219	33
PA5	C8/DAB/50%DAIS	14000	2.3	18100	2.4	221	37
PA6	C8/DAB/50%DAII	11900	2.0	14500	2.0	90	6
PA7	C8/DAIS[d]	-	-	4900	2.8	-	-
PA8	C8/DAH	39200	2.0	60200	2.6	227	54
PA9	C8/DAB/30%DAPIS	4200	2.3	6300	2.4	221/230	21
PA10	C8/DAH/30%DAPIS	8200	2.1	10500	2.6	202	26
PA11	C8/DAH/50%DAPIS	2600	2.2	5000	2.8	187	36
PA12	C8/DAPIS[d]	-	-	1300	1.4	128	138
PA13	C10/DAH	6500	2.1	10200	2.1	222	69
PA14	C10/DAB/30%DAPIS	3200	2.2	7300	2.3	189	46
PA15	C10/DAH/30%DAPIS	10200	2.2	12200	2.2	194	30
PA16	C10/DAH/50%DAPIS	7700	2.2	8000	2.6	186	33
PA17	C13/DAH	40200	2.0	86700	4.0	193	63
PA18	C13/DAB/30%DAPIS	4100	2.1	5200	2.2	184	23
PA19	C13/DAH/30%DAPIS	10300	2.1	12700	2.5	175	42
PA20	C13/DAH/50%DAPIS	7330	2.1	7400	2.2	152	47

[a]Determined by weighed-in monomers. [b]Determined for polyamides using SEC with PMMA standards in HFIP solvent. [c]Analyzed from the second DSC heating runs, T_m = melting point, ΔH_m = enthalpy of the transition during melting. [d]PA prepared via interfacial polymerization.

Results and Discussion

Synthesis and Molecular Characterization of the Polyamides. To prevent degradation of sugar-derived diamines during polymerization and to ensure sufficiently high molecular weight of the final products, low temperature melt polycondensation of nylon salts followed by solid-state polymerization have been applied. The majority of the reactions have been carried out under solvent-free conditions and representative results of the polymerizations are presented in Table 1.

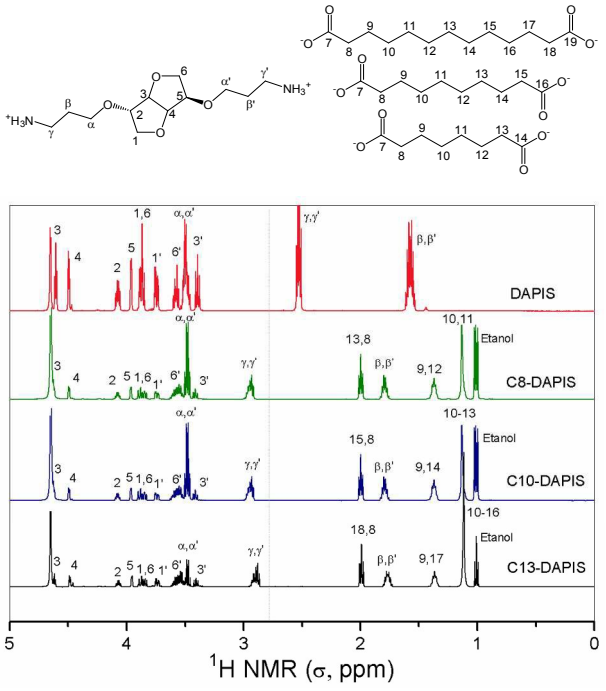

Figure 1. ^{1}H NMR spectra of DAPIS and C8-DAPIS, C10-DAPIS and C13-DAPIS nylon salts recorded in D_2O at ambient temperature.

Interfacial polymerization of bicyclic diamines resulted only in oligomers. Thiem and Bachmann[2] have also reported this phenomenon and assigned it to the sensitivity of the interfacial polymerization, which is strongly depending on temperature, type of organic solvent or molar ratio of the used monomers.

To compare the reactivity of primary and secondary isohexide-based diamines, a series of polymers have been prepared comprising of isosorbide(bis(propan-1-amine)) (DAPIS), diaminoisosorbide (DAIS), diaminoisoidide (DAII) and linear diamines *viz.* 1,4-diaminobutane (DAB), 1,6-diaminohexane (DAH) together with different dicarboxylic acids, having 6 to 11 methylene units between the acid functionalities. To guarantee proper thermal and mechanical properties of the polyamides, their targeted number average molecular weight should at least be 10,000 g/mol.[34] An increased degree of polymerization was observed by replacing DAB by DAH (Table 1, PA9 and PA10, PA14 and PA15, PA18 and PA19). Such an effect was visible for all samples containing C8, C10, and C13 dicarboxylic acids. We suspect that this may be caused by the cyclization of 1,4-diaminobutane end groups into pyrrolidine, preventing further polymerization.[32] The effect of an increasing contribution of DAPIS on the molecular weight and melting point of the polyamides was also studied (Table 1, e.g. PA10 and PA11). The presence of bicyclic diamines decreases the molecular weight and disorders the crystalline phase of the polymers, resulting in a lower melting point and enthalpy of the recorded transitions in comparison to the linear reference polymers containing the same dicarboxylic acids (entry PA1, PA8, PA13, and PA17 in Table 1). This, however, might facilitate the processing of the synthesized polyamides. DSC results show a proof of principle that the incorporation of isohexide-based diamines significantly affects the hydrogen bonding in the PAs, inducing less perfect chain packing in the polymers. The effect of replacing DAII and DAIS by DAPIS (Table 1, PA2, PA4, PA9) on the thermal properties of the copolyamides was also investigated. By exchanging the exo-endo oriented secondary diamine (DAIS) by a primary DAPIS, whilst maintaining a constant contribution of the bicyclic compound, a broader melting transition with significantly lower

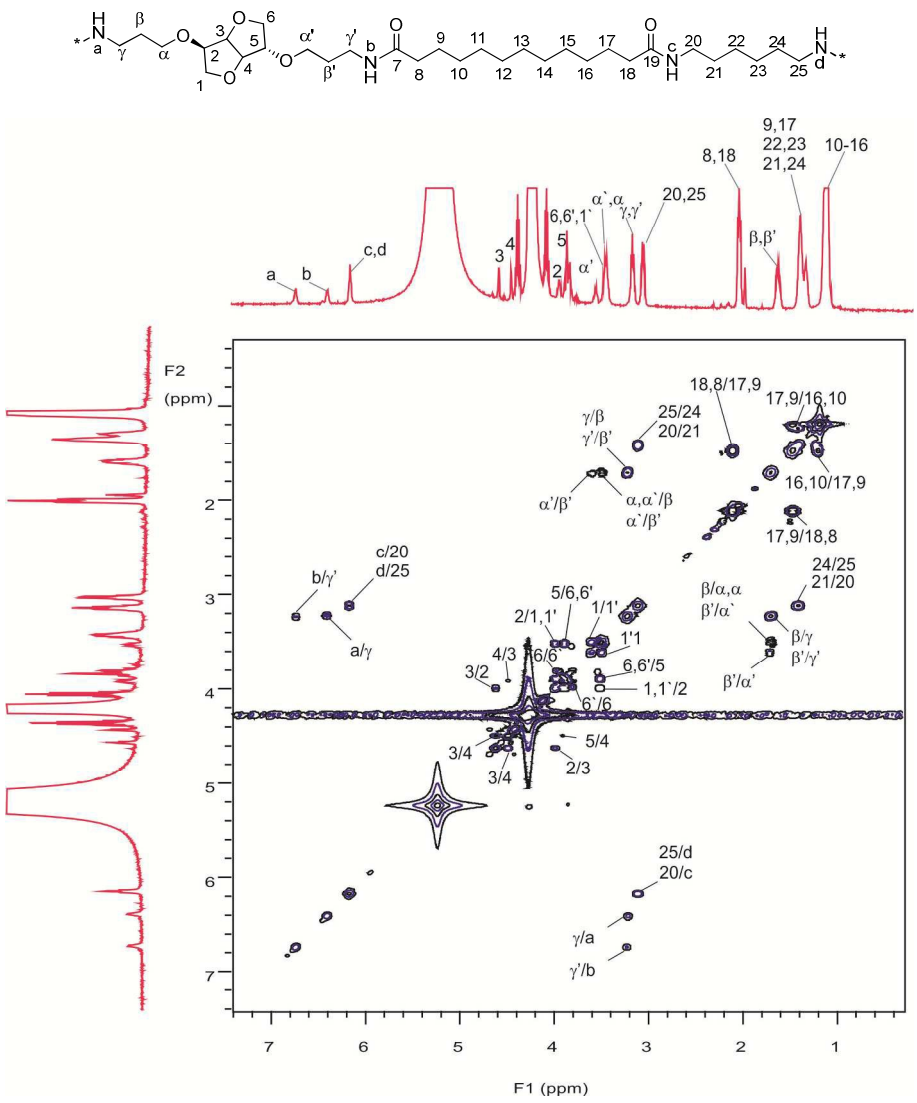

Figure 2. 500 MHz Correlation Spectra COSY of PA20 recorded in HFIP/C_6D_6 mixture at ambient temperature.

ΔH_m was observed. This indicates that the flexibility of DAPIS allows it to be more readily located in the crystalline phase of the polymer than the more rigid DAIS. In line with our previous work carried out for isohexide-based polyamides,[32-34] a decrease of the polymer's melting temperature with an increasing distance between amide groups was noted. An example of this phenomenon can be found in sebacic acid (C8)-based polyamides containing 30 wt % of DAPIS. The melting temperature of this polymer was 202 °C (PA10, Table 1), while the T_m of its brassylic acid (C13)-based analogue is only 175 °C (PA19, Table 1).

To elucidate the chemical structure of DAPIS-derived nylon salts and their incorporation into the corresponding copolymers, liquid-state 1D (^{1}H NMR) and 2D NMR (^{1}H-^{1}H COSY) experiments were employed. Figure 1 evidently demonstrates the formation of C8-DAPIS, C10-DAPIS, and C13-derived nylon salts. Upon reaction of DAPIS with the corresponding dicarboxylic acids, the signals assigned to the γ and γ' protons of the isohexide diamine present in the salt shift towards lower field. Similar trends are observed for the β and β' protons further supporting the quantitative conversion of the bicyclic diamine into the corresponding nylon salts. A more in-depth NMR analysis was carried out on the isohexide-derived polyamides. A representative 2D ^{1}H–^{1}H COSY spectrum of the polymer C13/DAH/DAPIS-based PA20 is presented in Figure 2. The preservation of the *exo-endo* configuration of DAPIS, incorporated into the polymer backbone, is confirmed by the two signals from the bridge-protons H3 and H4 at 4.62 and 4.51 ppm, respectively. As these protons are positioned close to H2 (4.10 ppm in the COSY spectrum) and H5 (3.94 ppm in the COSY spectrum) having an *endo* and *exo* configuration, two well-resolved signals related to H3 and H4 can be distinguished. Furthermore, the correlation signal of H6/H6' is found at 4.0 ppm, whilst the signal for H5/H6 is located at 3.97 ppm. Strikingly, well-resolved cross peaks Hα,α'/Hβ,β', Hγ,γ'/Hβ,β', Hβ,β'/Hγ,γ', proving the incorporation of DAPIS into the

polymer, are visible at 3.62–3.70 ppm, 3.22 ppm and 1.75 ppm, respectively. The signals from Ha, Hb, Hc, Hd at 6.75 ppm, 6.40 ppm and 6.18 ppm provide unambiguous confirmation of amide bond formation. The 2D ^{1}H–^{1}H COSY spectrum also includes signals assignable to linear chain fragments originating from DAH and BrA. These can be found around 1.0–2.2 ppm. For comparison, the 2D ^{1}H–^{1}H COSY spectrum of DAIS-based polyamide (PA5) and its corresponding assignments can be found in Figure S5.

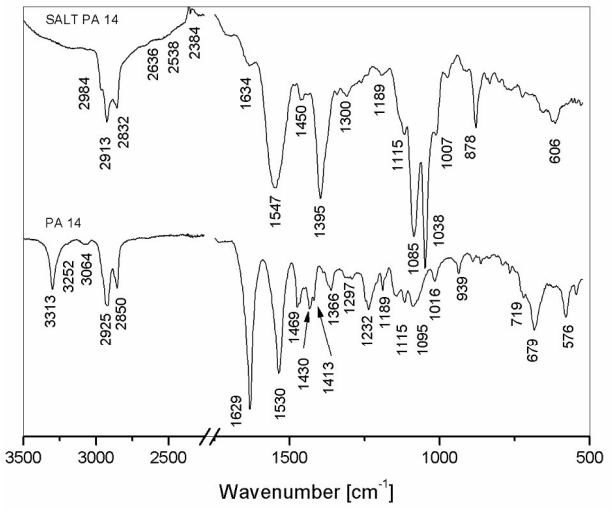

Figure 3. FT-IR spectra recorded for C10/DAPIS salt and PA14.

As shown above using liquid-state NMR, FT-IR spectra recorded for the nylon salts and polyamides confirm that isohexide diamines can be effectively polymerized or copolymerized under the applied reaction conditions. For example, the representative FT-IR spectra of the C10/DAPIS salt and of the corresponding polymer PA14 (Figure 3) clearly prove the effective formation of the polyamides. Table S1 in the Supporting Information summarizes the complete peak assignment. In the FT-IR spectra of Figure 3, the N-H stretching vibrations attributed to hydrogen bonded amide groups can be detected at 3300–3075 cm^{-1}. The bands derived from C-N stretching vibrations of the amide functional group appear at 1530, 1413 and 1189 cm^{-1}, respectively. Besides, the FT-IR spectra show the bands corresponding to C=O stretching vibrations of nylon salt at 1547 cm^{-1} and 1395 cm^{-1}, which upon polymerization move to 1630 cm^{-1} and 1440 cm^{-1}. Interestingly, FT-IR spectroscopy shows that the majority of methylene units occur in trans conformation. This is based on the bands at 1469 cm^{-1} and 1413 cm^{-1}, which derive from CH_2 scissoring vibrations next to an NH and CO having trans conformation,[34] at room temperature the presence of gauche conformers in the DAPIS-based samples can be neglected. Using the information provided by FT-IR spectroscopy one can conclude that the chemical structure of DAPIS does not significantly perturb the supramolecular arrangement of the linear polymer chain fragments. Combining these results from FT-IR spectroscopy with those from DSC (Figure S1-S4) show that DAPIS is able to incorporate into the crystalline phase of the polymers and at room temperature leaves the trans conformation of the polymer chain fragments unaffected. Further proof for the incorporation of DAPIS into the polyamides is provided by asymmetric C-O-C stretching bands at 1095 cm^{-1} and "crystalline" amide stretching vibrations of the bicyclic units visible at 939 cm^{-1}, respectively.[33]

Geometry optimization. DFT calculations were carried out for simplified models with terminal methoxy groups instead of 3-amino-propoxy groups attached to both sides of the cyclic unit. This approximation is based on assumption of minor importance of the alkoxy fragment of the DAPIS molecule for the interpretation of the experimental ^{13}C chemical shifts originating from the isohexide fragment. Moreover, in our conformational search we have replaced the ethoxy fragments by methoxy groups, since the remote exocyclic methylene and amine groups have little influence on the potential energy surface of the isohexide unit.

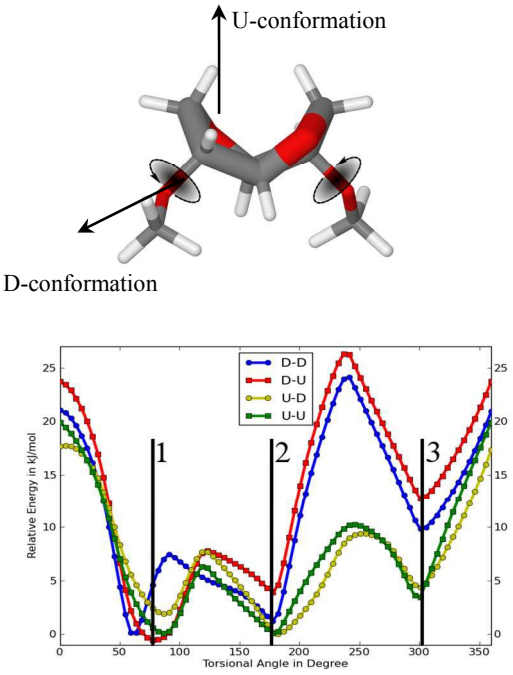

Figure 4. Conformational search scheme for the different boat and chair conformations (DD, DU, UD, and UU) of the DAPIS isohexide unit (upper part) and corresponding 1D potential energy plots (lower part).

The conformations of the isohexide moiety resemble the chair/boat-like conformations of cyclohexane. Following our previous work,[32,33,35] we have defined down-down (DD), down-up (DU), up-down (UD), and up-up (UU) conformations of the isohexide-moiety as illustrated in Figure 4. For each conformation (DD, DU, UD, UU) of the isohexide-moiety, the potential energy surface (PES) profiles have been calculated by varying the torsional angle between the isohexide-fragment and the methoxy group.

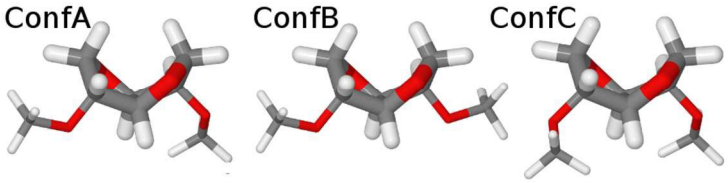

conformer	dE kJ/mol	abundance methylated derivatives	dE kJ/mol	abundance ethylated derivatives
ConfA	0	29%	0	33%
ConfB	0.62	22%	2.34	13%
ConfC	0.88	20%	0.57	26%
ConfD	1.65	15%	2.13	14%
ConfE	1.65	15%	2.3	13%

Figure 5. Structures of the most abundant conformers under ambient conditions according to Boltzmann's distribution based on Gibbs Free Energies analysis for the methylated (left) and ethylated (right) derivatives.

In order to prevent a low-barrier interconversion between DD-UU conformations during PES scans, the initial conformation of the isohexide-moiety was forcibly fixed as illustrated in Figure 4 using a solid wireframe representation. The variation of the torsional angle was performed in clockwise steps of 30° where, during the energy minimizations, the shape of the isohexide core was fixed, while the rest of the fragment was allowed to relax. The energy profiles were then used to prepare the 1D-PES plot (Figure 4), i.e., for each geometry and torsional angle the lowest energy conformation was selected for further re-optimization. Figure 4 clearly shows three minima, which correspond to a torsional angle of approximately 60°, 180°, and 300°. The abundance of the identified conformers was estimated by computing Boltzmann probabilities for each conformer at 25 °C.

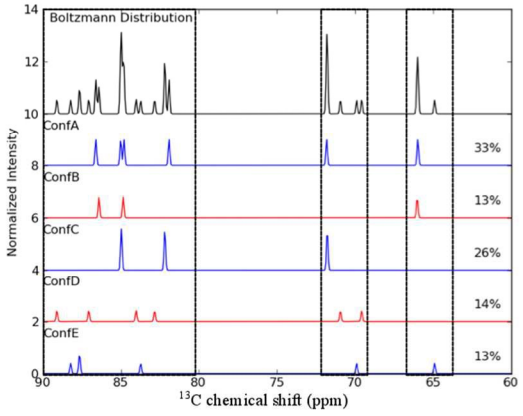

Figure 6. Graphical representation of the calculated ^{13}C NMR spectra for the five most abundant conformers of isohexide units present in the conformers A-E (see Figure 5) and total summarized ^{13}C NMR spectrum based on the Boltzmann distribution.

Applying an energy threshold of 5 kJ/mol, an extensive quantum-chemical conformational analysis via DFT-D method revealed five most abundant conformers. Based on these conformers it became evident that the isohexide-core energetically preferentially adopts UU (conformers A-C) and UD (conformers D-E) conformations as presented in Figure 5. The structures of conformers D and E were omitted in the presented figure as their spatial orientations of methoxy groups are identical to those in conformer A and C.

Local polymer chain conformation and mobility probed by solid-state NMR. All identified conformers summarized in Figure 5 were used for further NMR chemical shift calculations. It is worth mentioning that every conformer has shown noticeably different ^{13}C chemical shifts for the carbons of the cyclic unit (Figure 6), which is reflected in the population weighted ^{13}C NMR spectrum as a spread of peaks in the range of 60–90 ppm. However, this spread indicates that the corresponding experimental ^{13}C NMR spectrum should have significantly broadened ^{13}C resonances unless the conformational distribution will be dominated by one or two conformers, which can suddenly become significantly more favorable due to additional macroscopic factors such as packing effects, entropy, etc. Despite the spectral diversity of the isohexide-core, three characteristic regions at 65, 70, and 85 ppm can be separated that are suitable to be used for qualitative analysis of the conformation distribution of the isohexide units present in the polymer backbone. Based on our previous solid-state 2D NMR studies we learned that different isohexide conformers are able to form hydrogen bonds and contribute in the crystalline fraction of the materials.[32]

Variable temperature solid-state NMR spectroscopy was applied to provide information about the distribution of DAPIS between the polymer's amorphous and crystalline phase as well as to study the polymer chain mobility upon heating. To this end we have used solid-state ^{13}C{^{1}H} Cross-Polarization/Magic-Angle Spinning (CP/MAS) NMR and ^{13}C{^{1}H} Insensitive Nuclei Enhanced by Polarization Transfer (INEPT) experiments in parallel to gain detailed information about the flexible nature of the investigated polymers. We have here chosen to focus on the sample PA 20 (see Figure 7) having a significant contribution of DAPIS. The ^{13}C{^{1}H} CP/MAS NMR spectrum recorded at room temperature indicates that DAPIS units can adopt numerous

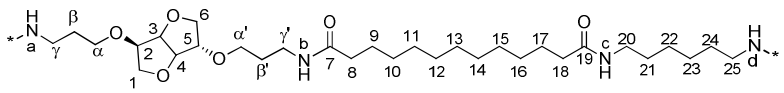

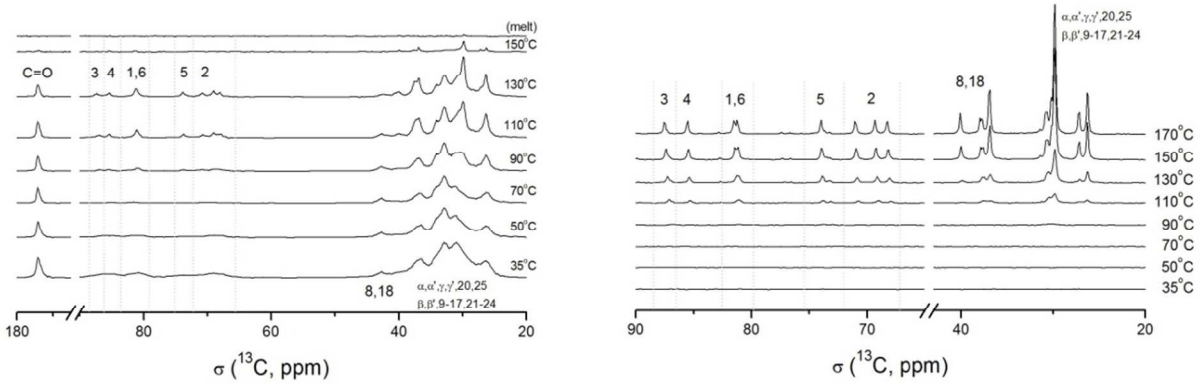

Figure 7. Variable-temperature solid-state (left) $^{13}C\{^{1}H\}$ CP/MAS NMR and (right) ^{13}C INEPT NMR spectra of PA20.

geometric conformations (see Figure 7, left side). The ^{13}C signals assigned to 1–6 for the bicyclic fragment of DAPIS are located in the region 65–90 ppm. The ^{13}C resonances corresponding to the linear moieties of brassylic acid, 1,6-diaminohexane, and the α, β, γ carbons of DAPIS are positioned between 20–50 ppm. Upon heating PA20, the line shapes of the ^{13}C resonances in the recorded spectra change significantly. More importantly, new ^{13}C signals corresponding to gauche conformers appear at 34 and 40 ppm. Above 110 °C, the ^{13}C resonances sharpen and become better resolved in comparison to those recorded at 35 °C. This difference indicates that the contribution of different conformers in the polymer backbone is temperature dependent and that at higher temperature above T_g of the polyamides a dynamic equilibrium of rapidly exchanging conformers exists. It is worth to mention that the presence of relatively broad resonances in the $^{13}C\{^{1}H\}$ CP/MAS NMR spectra is in line with our DFT calculations, i.e., these showed a collection of adjacent resonances corresponding to different DAPIS conformers. Furthermore, with increasing flexibility of the polymer chain fragments upon heating, the $^{13}C\{^{1}H\}$ CP/MAS NMR spectra reveal a significant intensity decay at temperatures above 130 °C. Specifically the signal of the carbonyl groups around 174 ppm, related to hydrogen bond density decrease, as reported for other isohexide-derived polyamides.[32,33,35] In parallel, to elucidate the increased flexibility of the polymer chains in the PA20 sample we have employed $^{13}C\{^{1}H\}$ INEPT to focus on ^{13}C signals with longer T_2-relaxation times (Figure 7). A close analysis of these spectra revealed numerous signals between 65–90 ppm and 25–40 ppm above 110 °C. These signals correspond to the cyclic units and linear chain fragments, respectively. Besides an increase in the gauche conformers population at elevated temperatures (Figure 7), the ^{13}C resonances corresponding to gauche conformers also sharpen in $^{13}C\{^{1}H\}$ INEPT spectra. These findings demonstrate an enhancement of the chain dynamics, especially for the amorphous phase of the copolyamides where gauche conformers are predominantly located.

The influence of sugar-derived moieties present in polymers backbone on thermal properties of the selected polyamides was investigated by TGA (Table 2, Figure S6).

Table 2. Thermal properties of linear polyamides (PA1, PA17) and selected copolyamides containing DAIS or DAPIS (PA 2, PA19, PA20).

entry	Composition	$T_{5\%}$ (°C)[a]	$T_{10\%}$ (°C)[a]	T_{max} (°C)[a]
PA1	C8/DAB	361	398	462
PA2	C8/DAB/30%DAIS	334	377	455
PA17	C13/DAH	406	422	456
PA19	C13/DAH/30%DAPIS	372	398	431
PA20	C13/DAH/50%DAPIS	365	391	428

[a] $T_{5\%}$ = temperature corresponding to 5% weight loss, $T_{10\%}$ = temperature corresponding to 10% weight loss, T_{max} = temperature corresponding to maximal rate of degradation

The first step of materials decomposition, described as 5 wt % of their weight loss, was found well above 300 °C. By comparing TGA profiles of linear polyamides PA1 and PA17 with the DAIS and DAPIS-based copolyamides PA2, PA19, PA20 (Figure S6) some lower thermal stability of the latter ones can be observed. The copolymers containing 30 wt% of DAIS or DAPIS revealed $T_{5\%}$ at around 330 °C and 370 °C, respectively. Further increase of the DAPIS content in the polymers (up to 50 wt%, PA 20 Table 2) did not diminish their thermal stability significantly. The first step of decomposition of PA 20 occurred at 365 °C. Here, it should be noted that the profound influence of the polyamides' thermal stability is not only caused by the content of the bicyclic diamine but also by the molecular weight of the materials. Still, the major decomposition of the investigated materials was found to be above 420 °C, which in view of their melting points demonstrates rather good thermal stability and processability.

Figure 8 shows the temperature variation of the storage modulus G' (solid lines) and tan δ (dotted lines) of PA1, PA2, PA17 and PA19. The profiles representing the storage modulus of the investigated polyamides reveal three characteristic regions *viz.* a glassy – high modulus region where the mobility of the polymers' backbone is restricted, a glass transition region with a visible decay of the G' values and finally a rubbery plateau. Taking into account significantly higher flexibility of C13/DAH-based polyamides in comparison to C8/DAB-derived polymers, a less

pronounced rubbery plateau and noticeable viscous region for PA17 and PA19 can be observed. Higher storage modulus of DAIS and DAPIS-based polyamides (PA2, PA19) in comparison to the linear reference polyamides (PA1, PA17) indicate that the incorporation of isohexides enhances stiffness of the materials.

Temperature dependence of the tan δ factor, represented in Figure 8 as dotted lines, defines the internal mechanical loss in the material and is closely related to the local maxima of G", which was used to determine the glass transition temperature of the samples (see Figure S7 and Table S2). The incorporation of 30 wt% of DAIS into the linear C8/DAB-based polyamides increased the T_g from -1.7 °C (PA1) to 14.1 °C (PA2). The same effect might have been expected for C13/DAH/DAPIS-derived materials. However, these polymers revealed a decay of T_g values upon incorporation of DAPIS from 14.3 °C (PA17) to 7.8 °C (PA19). This observation can be interpreted in view of Flory–Fox equation relating the T_g of the polymers to their molecular weight,[45] as the molecular weight of DAPIS-based PA19 (M_n = 12700 g/mol) is significantly lower in comparison to its linear reference PA17 (M_n = 86700 g/mol), explaining the dependence of T_g for the low molecular weight PA19 sample. A thorough analysis of the G" temperature variation exhibits typical local maxima corresponding to α, β and γ relaxation processes in the decreasing order of the temperature. As described before,[46] α-relaxation at the highest temperature corresponds to the glass transition temperature, β-relaxation results from the motions of amide polar groups while at around -130–140 °C typical γ-relaxation, associated with single relaxation process of the amorphous region, can be found.

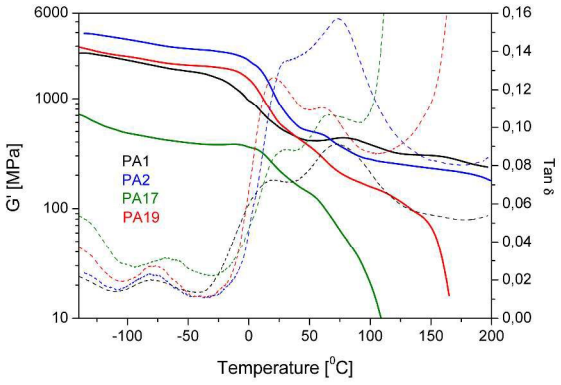

Figure 8. The storage modulus G` and the loss tangent tanδ as a function of temperature of PA1 (C8/DAB), PA2 (C8/DAB/30%DAIS), PA17 (C13/DAH), PA19 (C13/DAH/30%DAPIS).

Conclusions

This work has demonstrated that fully biobased polyamides revealing sufficiently high molecular weights and thermal stability containing isohexide units can be efficiently synthesized via low temperature bulk polycondensation followed by solid-state polymerization. Under the applied relatively mild conditions incorporation of the bicyclic diamines into the polymer backbone is quantitative without any degradation of the sugar derivatives. Polymers containing DAIS and DAPIS units revealed about 30–40 °C lower decomposition temperature in comparison to their linear references. FT-IR spectroscopy exhibited that a major part of the methylene groups present in the investigated copolyamides occur in a *trans* conformation, which is favorable in the crystalline phase of the samples. Furthermore, FT-IR and DSC analyses have shown that although isohexide derivatives reveal significantly different chemical structures than the linear diamines applied in our study, they can be incorporated into the crystal phase of the samples. DFT studies on an isohexide diether model compound revealed five most stable conformations for which the ^{13}C NMR spectra have been calculated. The simulated spectra helped to understand the shape and position of the resonances of the DAPIS units in the PAs recorded in the solid-state CP/MAS NMR and INEPT spectra. The experiments proved that changes of the conformer type together with an enhanced mobility of the macromolecules is already visible way below their melting point. DMTA revealed that the incorporation of isohexide units into the polymer backbone enhances stiffness of the materials especially at low temperature while the glass transition temperature is strongly driven by the composition and, for the rather low molecular weight samples studied here, by the polymer's molecular weight.

Notes and references

[a]*Department of Polymer Technology, Chemical Faculty, Gdansk University of Technology, G. Narutowicza Str. 11/12, 80-233 Gdansk, Poland,* [b]*Food & Biobased Research, Wageningen University and Research Center, Bornse Weilanden 9, 6708 WG Wageningen, The Netherlands,* [c]*Max Planck Institute for Polymer Research, Ackermannweg 10, 55128 Mainz, Germany,* [d]*Interdisciplinary Nanoscience Center (iNANO) and Department of Chemistry, Gustav Wieds Vej 14, DK-8000 Aarhus C, Denmark,* [e]*Laboratory of Polymer Chemistry, Eindhoven University of Technology, Den Dolech 2, P.O. Box 513, 5600 MB Eindhoven, The Netherlands.*

The financial support of Foundation for Polish Science (FNP; project HOMING PLUS/2012-5/2) is gratefully acknowledged.

† Electronic Supplementary Information (ESI) available: DSC, liquid-state 2D NMR, FT-IR, TGA, DMTA See DOI: 10.1039/b000000x/

* To whom correspondence should be addressed. e-mail: l.jasinska@tue.nl, r.duchateau@tue.nl

1. Grimme, J. *Comp. Chem.* 2006, **27**, 1787–1799.
2. Thiem, J.; Bachmann, F. *Makromol. Chem.* 1991, **192**, 2163–2182.
3. Thiem, J.; Leuders, H. *Makromol. Chem.* 1986, **192**, 2775–2785.
4. Okada, M.; Okada, Y.; Aoi, K. *J. Polym. Sci. Part A Polym. Chem.* 1995, **33**, 2813–2820.
5. Okada, M.; Okada, Y.; Tao, A.; Aoi, K. *J. Appl. Polym. Sci.* 1996, **62**, 2257–2265.
6. Okada, M.; Tsuonoda, K.; Tachikawa, K.; Aoi, K. *J. Appl. Polym. Sci.* 2000, **77**, 338–346.
7. Storbeck, R.; Ballauff, M. *J. Appl. Polym. Sci.* 1996, **59**, 1199–1202.
8. Gubbels, E.; Jasinska-Walc, L.; Koning, C. E. *J. Polym. Sci. Part A: Polym. Chem.* 2013, **51**, 890–898.
9. Gubbels, E.; Jasinska-Walc, L.; Noordover, B. A. J.; Koning, C. E. *Eur. Polym. J.* 2013, **49**, 3188–3198.
10. Charbonneau, L. F.; Johnson, R. E.; Khanarian, G.; Lee, R. G.; Nelson, G. V.; Sandor, R. B.; Witteler, H. B. WO 1999054129, 2000.
11. East, A.; Jaffe, M.; Zhang, Y.; Catalani, L. US 7619056, 2008.
12. Gillet, J. P. FR 2915483, 2008.
13. Wu, J.; Eduard, P.; Thiyagarajan, S.; van Haveren, J., van Es, D. S.; Koning, C. E.; Lutz, M.; Fonseca Guerra, C. *ChemSusChem.* 2011, **4**, 599–603.
14. Okada, M.; Yamada, M.; Yokoe, M. *J. Appl. Polym. Sci.* 2001, **81**, 2721–2734.
15. Wu, J.; Eduard, P.; Thiyagarajan, S.; Jasinska-Walc, L.; Rozanski, A.; Fonseca Guerra, C.; Noordover, B. A. J.; van Haveren, J.; van Es, D. S.; Koning, C. E. *Macromolecules* 2012, **45**, 5069–5080.

16. Wu, J.; Eduard, P.; Jasinska-Walc, L.; Rozanski, A.; Noordover, B. A. J.; van Es, D. S.; Koning, C. E. *Macromolecules* 2013, **46**, 384–394.
17. Philip, B.; Sreekuram, K. *Polym. Int.* 2001, **50**, 1318–1323.
18. Gorna, K.; Gogolewski, S. *J. Biomed. Mater. Re. Part A.* 2006, **79**, 128–138.
19. Fenouillot, F.; Rousseau, A.; Colomines, G.; Saint-Loup, R.; Pascault, J. P. *Prog. Polym. Sci.* 2010, **35**, 578–622.
20. Duchateau, R.; van Meerendonk, W. J.; Staal, B. B. P.; Koning, C. E.; Gruter, G. *Macromolecules* 2006, **39**, 7900–7908.
21. Thiyagarajan, S.; Gootjes, L.; Vogelzang, W.; Wua, J.; van Haveren, J.; van Es, D. S. *Tetrahedron* 2011, **67**, 383–389.
22. Bachmann, F.; Reimer, J.; Ruppenstein, M.; Thiem, J. *Macromol. Chem. Phys.* 2001, **202**, 3410–3419.
23. Pfeffer, J.; Ortelt, M.; Spyrou, E.; Haas, T.; Korek, U.; Schmidt, H.; Dingerdissen, U. WO 2011000585, 2011.
24. Japu, C.; Alla, A.; Martinez de Ilarduya, A.; Garcia-Martín, M.; Benito, E.; Galbis, J. A.; Munoz-Guerra, S. Polym. Chem. 2012, 3, 2092-2101.
25. Lavilla, C.; Martinez de Ilarduya, A.; Alla, A.; Munoz-Guerra, S. Polym. Chem. 2013, 4, 282-289.
26. Lavilla, C.; Martinez de Ilarduya, A.; Alla, A.; Garcia-Martin, M. G.; Galbis, J. A.; Munoz-Guerra, S. *Macromolecules,* 2012, **45**, 8257-8266.
27. Lavilla, C.; Alla, A.; Martinez de Ilarduya, A.; Benito, E.; Garcia-Martin; M.G.; Galbis, J.A.; Munoz-Guerra, S. *Polymer*, 2012, **53**, 3432-3445.
28. Lavilla, C.; Alla, A.; Martinez de Ilarduya, A.; Munoz-Guerra, S. *Biomacromolecules,* 2013, **14**, 781-793.
29. Lavilla, C.; Gubbels, E.; Martinez de Ilarduya, A.; Noordover, B. A.; Koning, C. E.; A.; Munoz-Guerra, S. *Macromolecules,* 2013, **46**, 4335-4345.
30. Gubbels, E.; Lavilla, C.; Martinez de Ilarduya, A.; Noordover, B. A.; Koning, C. E.; A.; Munoz-Guerra, S. *J. Polym. Sci. Part A: Polym. Chem.* 2014, **52**, 164-177.
31. Caouthar, A. A.; Loupy, A.; Bortolussi, M.; Blais, J. C.; Dubreucq, L.; Meddour, A. *J. Polym. Sci. Part A: Polym. Chem.* 2005, **43**, 2480–2491.
32. Jasinska-Walc, L.; Dudenko, D.; Rozanski, A.; Thiyagarajan, S.; Sowinski, P.; van Es, D. S.; Koning, C. E. *Macromolecules* 2012, **45**, 5653–5666.
33. Jasinska-Walc, L.; Villani, M.; Dudenko, D.; van Asselen, O.; Klop, E.; Rastogi, S.; Hansen, M. R.; Koning, C. E. *Macromolecules* 2012, **45**, 2796–2808.
34. Jasinska, L.; Villani, M.; Wu, J.; van Es, D. S.; Klop, E.; Rastogi, S.; Koning, C. E. *Macromolecules* 2011, **44**, 3458–3466.
35. Wu, L.; Jasinska-Walc, L.; Dudenko, D.; Rozanski, A.; Hansen, M. R.; van Es, D. S.; Koning, C. E. *Macromolecules* 2012, **45**, 9333–9346.
36. Thiyagarajan, S.; Gootjes, L.; Vogelzang, W.; van Haveren, J.; Lutz, M.; van Es, D. S. *ChemSusChem* 2011, **4**, 1823–1829.
37. (a) Frisch, M. J. Gaussian 09 Revision A. 02; Gaussian, Inc.: Wallingford, CT, 2009. (b) Grimme, S. *J. Comput. Chem.* 2006, **27**, 1787–1799.
38. Morris, G. A.; Freeman, R. *J. Am. Chem. Soc.* 1979, **101**, 760–762.
39. Burum, D. P.; Ernst, R. R. *J. Magn. Reson.* 1980, **39**, 163–168.
40. Doddrell, D. M.; Pegg, D. T.; Bendall, M. R. *J. Magn. Reson.* 1982, **48**, 323–327.
41. Saalwächter, K.; Lange, F.; Matyjaszewski, K.; Huang, C. F.; Graf, R. *J. Magn. Reson.* 2011, **212**, 204–215.
42. Saalwächter, K. *Prog. Nucl. Magn. Reson. Spectrosc.* 2007, **51**, 1–35.
43. Morcombe, C. R.; Zilm, K. W. *J. Magn. Reson.* 2003, **162**, 479–486.
44. Hayashi, S.; Hayamizu, K. B. *Bull. Chem. Soc. Jpn.* 1991, **64**, 685−687.
45. Fox Jr., T. G.; Flory, P. J.; J. *J. Appl. Phys.* 1950, **21**, 581-591.
46. Jeziorska, R.; Swierz-Motysia, B.; Szadkowska, A.; Marciniec, B.; Maciejewski, H.; Dutkiewiecz, M.; Leszczynska, I. *Polimery* 2001, **56**, 809-816.